Human Topoisomerase I Poisoning by Protoberberines: Potential Roles for Both Drug−DNA and Drug−Enzyme Interactions†

Tsai-Kun Li,‡ Eleanor Bathory,§ Edmond J. LaVoie,|| A. R. Srinivasan,§ Wilma K. Olson,§,⊥ Ronald R. Sauers,§ Leroy F. Liu,‡,⊥ and Daniel S. Pilch*,‡,⊥

Department of Pharmacology, University of Medicine and Dentistry of New Jersey, Robert Wood Johnson Medical School, 675 Hoes Lane, Piscataway, New Jersey 08854, Departments of Chemistry and Pharmaceutical Chemistry, Rutgers−The State University of New Jersey, Piscataway, New Jersey 08854, and The Cancer Institute of New Jersey, New Brunswick, New Jersey 08901

Received January 31, 2000; Revised Manuscript Received April 14, 2000

ABSTRACT: Protoberberines represent a structural class of organic cations that induce topoisomerase I-mediated DNA cleavage, a behavior termed topoisomerase I poisoning. We have employed a broad range of biophysical, biochemical, and computer modeling techniques to characterize and cross-correlate the DNA-binding and topoisomerase poisoning properties of four protoberberine analogues that differ with respect to the substituents on their A- and/or D-rings. Our data reveal the following significant features: (i) The binding of the four protoberberines unwinds duplex DNA by approximately 11°, an observation consistent with an intercalative mode of interaction. (ii) Enthalpically favorable interactions, such as stacking interactions between the intercalated ligand and the neighboring base pairs, provide <50% of the thermodynamic driving force for the complexation of the protoberberines to duplex DNA. Computer modeling studies on protoberberine−DNA complexes suggest that only rings C and D intercalate into the host DNA helix, while rings A and B protrude out of the helix interior into the minor groove. (iii) All four protoberberine analogues are topoisomerase I-specific poisons, exhibiting little or no topoisomerase II poisoning activity. (iv) Modifications of the D-ring influence both DNA binding and topoisomerase I poisoning properties. Specifically, transference of a methoxy substituent from the 11- to the 9-position diminishes both DNA binding affinity and topoisomerase I poisoning activity, an observation suggesting that DNA binding is important in the poisoning of topoisomerase I by protoberberines. (v) Modifications of the A-ring have a negligible impact on DNA binding affinity, while exerting a profound influence on topoisomerase I poisoning activity. Specifically, protoberberine analogues containing either 2,3-dimethoxy; 3,4-dimethoxy; or 3,4-methylenedioxy substituents all bind DNA with a similar affinity. By contrast, these analogues exhibit markedly different topoisomerase I poisoning activities, with these activities following the hierarchy: 3,4-methylenedioxy > 2,3-dimethoxy ≫ 3,4-dimethoxy. These differences in topoisomerase I poisoning activity may reflect the differing abilities of the analogues to interact with specific functionalities on the enzyme, thereby stabilizing the enzyme in its cleavable state. In the aggregate, our results are consistent with a mechanistic model in which both ligand−DNA and ligand−enzyme interactions are important for the poisoning of topoisomerase I by protoberberines, with the DNA-directed interactions involving ring D and the enzyme-directed interactions involving ring A. It is reasonable to suggest that the poisoning of topoisomerase I by a broad range of other naturally occurring and synthetic ligands may entail a similar mechanism.

The antineoplastic activity exhibited by the camptothecin (CPT)[1] family of compounds against a broad spectrum of solid tumors has highlighted topoisomerase I (TOP1) as an attractive molecular target for anticancer drugs (*1*). The cytotoxic activities of these compounds are derived from their abilities to inhibit the religation step of the TOP1 reaction, thereby resulting in the accumulation of a ternary, DNA-cleavable complex that includes the drug, the enzyme, and the DNA (*2*−*4*). The Liu and Pommier groups have shown that CPT binds to the TOP1−DNA interface, while exhibiting little or no affinity for the enzyme or the DNA alone (*2*, *5*, *6*).

† This work was supported by grants from the National Institutes of Health [CA39962 (D.S.P. and L.F.L.) and GM20861 (W.K.O.)], the American Cancer Society [RPG CDD-98334 (D.S.P.)], and the New Jersey Commission on Cancer Research [00-64-CCR-S-0 (D.S.P.)].

* To whom correspondence should be addressed at Department of Pharmacology, UMDNJ-Robert Wood Johnson Medical School, 675 Hoes Lane, Piscataway, NJ 08854-5635. Telephone: 732-445-3954. Fax: 732-445-5312. E-mail: pilch@rutchem.rutgers.edu.

‡ UMDNJ-Robert Wood Johnson Medical School.

§ Rutgers University, Department of Chemistry.

|| Rutgers University, Department of Pharmaceutical Chemistry.

⊥ Cancer Institute of New Jersey.

[1] Abbreviations: TOP, topoisomerase; ST, salmon testes; 231011TM, 5,6-dihydro-2,3,10,11-tetramethoxydibenzo[*a,g*]quinolizinium; 341011TM, 5,6-dihydro-3,4,10,11-tetramethoxydibenzo[*a,g*]quinolizinium; 34MD1011DM, 5,6-dihydro-3,4-methylenedioxy-10,11-dimethoxydibenzo[*a,g*]quinolizinium; CPT, camptothecin; EtBr, ethidium bromide; PrI, propidium iodide; EDTA, disodium salt of ethylenediamintetraacetic acid; bp, base pair(s); r_{bp}, ratio of [total ligand] to [base pairs]; WC, Watson−Crick; T_m, melting temperature; ITC, isothermal titration calorimetry; DSC, differential scanning calorimetry.

10.1021/bi000171g CCC: $19.00
Published on Web 05/18/2000

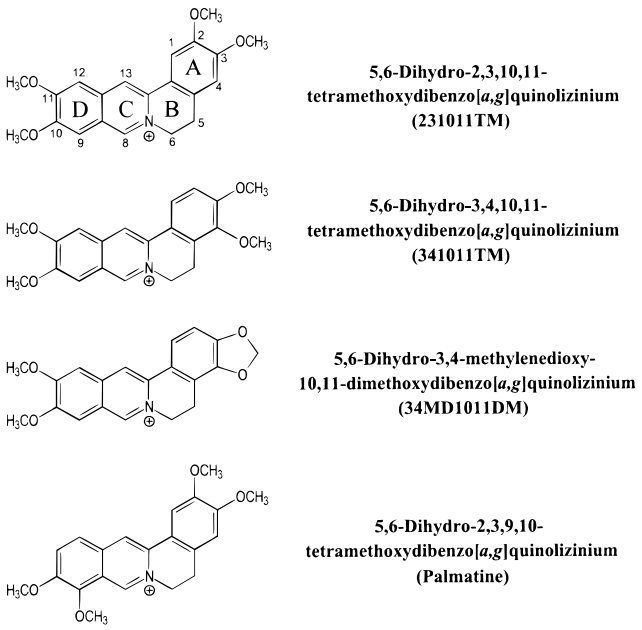

FIGURE 1: Chemical structures of 231011TM, 341011TM, 34MD1011DM, and palmatine. Atomic numbering and ring lettering are indicated in the structure of 231011TM (top).

In recent years, numerous other families of naturally occurring and synthetic compounds have been identified as TOP1 poisons (reviewed in ref *7*). In marked contrast to CPT, many of these compounds are known DNA binders (*7*). For drugs that target topoisomerase II (TOP2), drug intercalation into the host DNA duplex is strongly correlated with enzyme poisoning (*8*). However, the role, if any, that DNA binding plays in the drug-induced poisoning of TOP1 is unclear. To broaden our base of knowledge of the role that ligand−DNA interactions play in TOP1 poisoning, we have begun a program in which we are characterizing and cross-correlating the TOP1 poisoning and DNA-binding properties of various families of structurally related DNA-binding ligands. One of these families of compounds is the protoberberines. The protoberberines are organic cations that are structurally related to the plant alkaloids berberine and palmatine (reviewed in ref *9*). Previously, we reported that the binding of protoberberines to DNA is an important component of their TOP1 poisoning activities (*10*).

In this work, we evaluate whether DNA binding alone is sufficient to impart protoberberines with the ability to poison TOP1. Specifically, we characterize and cross-correlate the TOP1 poisoning and DNA-binding properties of the following four protoberberine analogues (see structures in Figure 1): 5,6-dihydro-2,3,10,11-tetramethoxydibenzo[*a,g*]quinolizinium (231011TM); 5,6-dihydro-3,4,10,11-tetramethoxydibenzo[*a,g*]quinolizinium (341011TM); 5,6-dihydro-3,4-methylenedioxy-10,11-dimethoxydibenzo[*a,g*]quinolizinium (34MD1011DM); and palmatine (5,6-dihydro-2,3,9,-10-tetramethoxydibenzo[*a,g*]quinolizinium). These four analogues differ with respect to the chemical substituents on their A- and/or D-rings. Our DNA binding data reveal that the protoberberines intercalate into duplex DNA while unwinding the host DNA by ≈11°. In addition, we show that modifications of the D-ring alter both DNA binding affinity and TOP1 poisoning activity, an observation consistent with our previous report (*10*) noting a correlation between these two properties. We also show that modifications of the A-ring have a negligible impact on DNA binding affinity while exerting a profound influence on TOP1 poisoning activity. These structure−activity relationships are consistent with a model for TOP1 poisoning by protoberberines in which both drug−DNA and drug−enzyme interactions are necessary for stabilization of the ternary (TOP1−DNA−drug) cleavable complex. It is reasonable to suggest that an ensemble of both drug−DNA and drug−enzyme interactions may be of general importance for drug-induced poisoning of TOP1.

MATERIALS AND METHODS

Enzyme, DNA, and Ligand Molecules. Recombinant human DNA topoisomerase I (hTOP1) was isolated from *E. coli* BL21(DE3) as described previously (*11*). Salmon testes (ST) DNA was obtained from Sigma Chemical Co. (St. Louis, MO), while ΦX-174 RF I DNA was obtained from Amersham Pharmacia Biotech (Piscataway, NJ). Both DNAs were used without further purification. The concentrations of all ST and ΦX-174 RF I DNA solutions were determined spectrophotometrically by assuming that one A_{260} unit/mL of DNA corresponds to a concentration of 50 μg/mL. pBluescript SK DNA was obtained from Stratagene (La Jolla, CA) and was purified as described previously (*8*). Palmatine was obtained from Aldrich Chemical Co. (Milwaukee, WI), while ethidium bromide (EtBr) was obtained from Sigma Chemical Co. CPT was obtained from the Drug Synthesis and Chemistry Branch of the Division of Cancer Treatment at the National Cancer Institute (Bethesda, MD), while teniposide (VM-26) was a generous gift from Bristol-Myers-Squibb (Lawrenceville, NJ). 231011TM, 341011TM, and 34MD1011DM were synthesized as described previously (*12*, *13*).

Topoisomerase Cleavage Assays. Topoisomerase cleavage assays were conducted as previously reported (*2*, *8*, *14*). The plasmid, YEpG, was linearized with *Bam*H1 and 3′-end labeled as previously described (*14*).

DNA Unwinding Assay. The DNA unwinding assay used to measure the relative strength of DNA intercalation was conducted in essentially the same manner as described previously (*8*) using a mixture of supercoiled and relaxed pBluescript SK DNA as substrates. Electrophoresis was performed at room temperature in buffer containing 40 mM Tris-phosphate (pH 8.3) and 1 mM EDTA (0.5× TPE buffer). Inhibition of TOP1 catalytic activity by the DNA-binding ligands, if present, is revealed by the presence of two groups of bands rather than a single Gaussian distribution of topoisomers.

Viscometry. Viscosity measurements were conducted in a Cannon-Manning size 75 capillary viscometer (Thomas Scientific, Swedesboro, NJ) submerged in a water bath that was maintained at 25.7 ± 0.1 °C. Flow times were measured two to three times to an accuracy of ±0.2 s with a stopwatch, and the average time over all replicates was recorded. Viscosity experiments were conducted at pH 6.1 in buffer containing 1.3 mM Tris-HCl, 5 mM sodium cacodylate, and 0.2 mM EDTA. Four microliter aliquots of either 150 μM EtBr or 600 μM protoberberine were titrated directly into the viscometer containing a solution (1 mL) of 200 μM nucleotide ΦX-174 RF I DNA, and flow times in the range of 117 to 137 s were measured after each addition.

UV Spectrophotometry. All UV absorbance experiments were conducted on an AVIV model 14DS spectrophotometer (Aviv Associates; Lakewood, NJ) equipped with a thermoelectrically controlled cell holder. A quartz cell with a 1-cm path length was used for all the absorbance studies. Absorbance versus temperature profiles were measured at 260 nm in CE buffer [5 mM sodium cacodylate (pH 7.0) and 0.1 mM EDTA] with a 5 s averaging time. The temperature was raised in 0.5 °C increments, and the samples were allowed to equilibrate for 1 min at each temperature setting. For each optically detected transition, the melting temperature (T_m) was determined as described previously (*15*). The DNA concentrations were 15 μM in base pair, while the ligand concentrations ranged from 0 to 7.5 μM.

Differential Scanning Calorimetry (DSC). Heat capacity (ΔC_p) versus temperature (T) profiles for the thermally induced transition of a solution containing 200 μM bp ST DNA were measured in CE buffer using a model 5100 Nano Differential Scanning calorimeter (Calorimetry Science Corporation; Provo, UT). In these experiments, the heating rate was 1 °C/min. The transition enthalpy (ΔH_{WC}) was calculated from the area under the heat capacity curve using the Origin version 4.1 software (MicroCal, Inc.; Northampton, MA).

Isothermal Titration Calorimetry (ITC). Isothermal calorimetric measurements were performed at 20 °C on a MicroCal MCS Titration Calorimeter (MicroCal, Inc., Northampton, MA). In a typical experiment, 5-μL aliquots of 500 μM ligand were injected from a 100-μL rotating syringe into an isothermal sample chamber containing 1.31 mL of a ST DNA solution that was 200 μM in base pair. The duration of each injection was 5.9 s, and the delay between injections was 300 s. The initial delay prior to the first injection was 60 s. Each injection generated a heat burst curve (μcal/s vs s). The area under each curve was determined by integration [using the Origin version 4.1 software (MicroCal, Inc., Northampton, MA)] to obtain a measure of the heat of ligand binding for that injection. The calorimeter was calibrated both electronically and chemically as described previously (*16*, *17*). All ITC experiments were conducted in CE buffer.

Computer Modeling. Models for the structures of 231011TM, 341011TM, 34MD1011DM, and palmatine were derived using the MacroModel version 5.0 software and the AMBER* force field (*18*). The resulting structures were used in subsequent studies aimed at modeling the complexes formed by these ligands and the host $d(ApT)_n-d(TpA)_n$ duplex. These modeling studies were conducted in two stages. The first stage entailed the identification of low energy duplex conformations, in which adjacent base pairs were separated sufficiently so as to accommodate insertion of a protoberberine molecule. A constrained molecular modeling method (*19*) was used to construct the duplex. The coordinates for Watson−Crick base pairs in a standard B-DNA conformation were used as the starting point of the calculations (*20*). Possible polymer building blocks that connect successive bases on each of the two strands then were identified by an exhaustive search of chain backbone conformation space. In all duplex structures, the base pair rise was set to 6.8 Å, a value that falls within the limits of the known geometries of drug−nucleic acid intercalation complexes (*21*), and the helical twist angle was set to 25°.

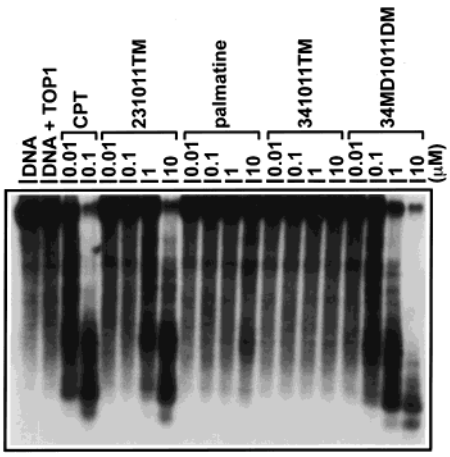

FIGURE 2: Human topoisomerase I-mediated DNA cleavage in the presence of the protoberberines and CPT (camptothecin). Agarose gel showing TOP1-mediated DNA cleavage, with the ligands and their concentrations (in units of micromolar) indicated at the tops of the lanes. Following incubation with both TOP1 and ligand, the DNA samples were treated with SDS and proteinase K and then alkali-denatured prior to loading on to a 0.8% agarose gel in 0.5× TPE buffer.

This twist angle reflects the protoberberine-induced duplex unwinding angle of 11° revealed by the viscosity studies reported here.

The unbound polymer duplex of lowest computed potential energy then was used in positioning the protoberberine molecule in the second stage of modeling. The coordinates of the protoberberine molecule were transformed to a reference frame in which the $x-y$ plane coincided with the plane formed by rings C and D of the ligand (see Figure 1). Initially, the ligand was placed halfway between the reference base pair and its neighbor in the duplex model. Numerous structures were generated by rotating the protoberberine molecule about the x, y, and z axes, as well as by translations along the x and y axes. Rotations about the z axis were varied in 10° intervals from 0 to 350°. Rotations about the x and y axes, which are analogous to the rolling and tilting motions of a standard Watson−Crick base pair in a B-DNA duplex, were varied in 5° intervals from −10 to +10°. The x and y translations were varied in 1 Å increments from −6 to +6 Å. These rotations and translations facilitated the identification of an energetically stable location for the intercalating ligand within the rigid duplex framework. At each ligand position, the potential energy of the ligand−duplex complex was determined using a standard potential energy function in which both repulsive and attractive van der Waals' contributions were estimated by a 6−12 potential (*22*, *23*).

RESULTS

The Extent to Which the Protoberberine Analogues Stimulate Human TOP1-Mediated DNA Cleavage Depends on the Nature of the Chemical Substituents on the A- and/or D-Rings. We compared the abilities of 231011TM, 341011TM, 34MD1011DM, and palmatine to poison human TOP1 by measuring the relative extents to which they stimulate TOP1-mediated cleavage of end-labeled YEpG DNA (Figure 2). The DNA was incubated with various concentrations of ligand in the presence of TOP1, and then was alkali-denatured prior to gel electrophoresis. This procedure reveals single-strand DNA breaks at specific sites on the DNA, with

the resulting DNA cleavage fragments appearing as fast-migrating species in the gel. Note that 231011TM and 34MD1011DM stimulate TOP1-mediated DNA cleavage in a manner dependent on their concentrations. By contrast, over an identical range of ligand concentrations, neither palmatine nor 341011TM stimulates TOP1-mediated DNA cleavage to a level significantly above the background. Further note that a 231011TM concentration of 10 μM is required to induce the same approximate level of TOP1-mediated DNA cleavage induced by 34MD1011DM at a concentration of only 1 μM. Thus, 34MD1011DM is a roughly 10-fold more potent stimulator of TOP1-mediated DNA cleavage than 231011TM. In the aggregate, our results indicate that the TOP1 poisoning capacities of the four protoberberine analogues studied here follow the hierarchy: 34MD1011DM > 231011TM $\gg$ palmatine $\approx$ 34MD1011DM.

Further inspection of Figure 2 reveals that even at a concentration of 1 μM, none of the four protoberberines stimulates TOP1-mediated DNA cleavage to the extent induced by only 0.1 μM of CPT. Thus, under the conditions used in these experiments, CPT is at least 10-fold more effective at poisoning TOP1 than any of the protoberberine analogues studied here.

Neither of the Four Protoberberine Analogues Stimulates TOP2-Mediated DNA Cleavage. We compared the abilities of 231011TM, 341011TM, 34MD1011DM, and palmatine to poison the alpha isozyme of human TOP2 by measuring the relative extents to which they stimulate TOP2-mediated DNA cleavage. These measurements (not shown) revealed that none of the protoberberine analogues stimulated TOP2-mediated DNA cleavage above the background level, an observation indicating that these four compounds are not TOP2 poisons. The lack of TOP2 poisoning activity exhibited by 341011TM and palmatine echoes their minimal abilities to poison TOP1 (Figure 2). However, the inability of 231011TM and 34MD1011DM to poison TOP2 contrasts with their potent TOP1 poisoning activities (Figure 2). This specificity for TOP1 versus TOP2 poisoning by 231011TM and 34MD1011DM may be correlated with their mode of DNA binding, which, as discussed below, exhibits properties characteristic of intercalation. The intercalated drug molecule may be accommodated sterically by TOP1 but not by TOP2, thereby precluding the stabilization of TOP2 in its cleavable state.

All Four Protoberberine Analogues Unwind Duplex DNA. DNA unwinding measurements were conducted to assess the impact, if any, of 231011TM, 341011TM, 34MD1011DM, and palmatine on the superhelical state of circular duplex DNA. The resulting unwinding profiles are shown in Figure 3. Note that each of the protoberberines induces a single Gaussian distribution of topoisomers, an observation indicating that, under the assay conditions employed, the ligands are not inhibiting the catalytic activity of TOP1 (i.e., the TOP1 poisoning activity is in excess, and thermodynamic equilibrium has been achieved). In these experiments, ligand-induced DNA unwinding is revealed by an upward and subsequent downward shift in the mobilities of the Gaussian centers of the topoisomers as a function of an increasing ligand concentration. Inspection of Figure 3 reveals that all four protoberberine analogues unwind duplex DNA in a concentration-dependent manner, an observation consistent with an intercalative mode of DNA binding. Furthermore,

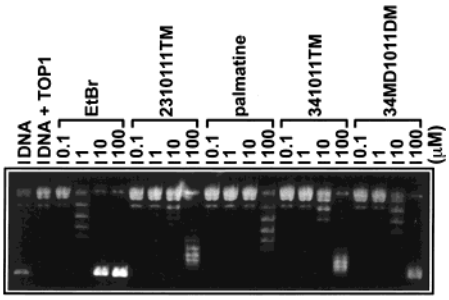

FIGURE 3: Agarose gel showing DNA duplex unwinding by the protoberberines and ethidium bromide (EtBr) in the presence of human TOP1. Ligands and their concentrations (in units of micromolar) are indicated at the tops of the lanes.

Table 1: ΔT_m-Derived Binding Affinities of 231011TM, 341011TM, 34MD1011DM, and Palmatine for Salmon Testes DNA at 25 °C[a]

ligand	T_{m0}[b] (°C)	T_m[b] (°C)	K_{25}[c] (M^{-1})
231011TM	61.4 ± 0.1	67.7 ± 0.1	(2.4 ± 0.3) × 10^5
341011TM	61.4 ± 0.1	67.2 ± 0.1	(2.5 ± 0.3) × 10^5
34MD1011DM	61.4 ± 0.1	67.3 ± 0.1	(2.3 ± 0.3) × 10^5
palmatine	61.4 ± 0.1	64.3 ± 0.1	(7.9 ± 1.3) × 10^4

[a] Solution conditions were 5 mM sodium cacodylate (pH 7.0) and 0.1 mM EDTA. [b] T_m values were derived from UV melting profiles at 15 μM base pair (bp) in the absence (T_{m0}) and presence of drug at a [total drug] to [base pair] ratio (r_{bp}) of 0.5. Each T_m value is an average derived from at least two independent experiments, with the indicated errors corresponding to the standard deviation from the mean. [c] Binding constants at 25 °C (K_{25}) were determined using eqs 2 and 3, the appropriate values of ΔH_b listed in Table 2, and a calorimetrically determined (see Materials and Methods) duplex-to-single strand transition enthalpy (ΔH_{WC}) of 7.2 kcal/mol bp for salmon testes DNA. Indicated uncertainties reflect the maximum errors in K_{25} that result from the corresponding uncertainties noted above in T_{m0}, T_m, and ΔH_b, as propagated through eqs 2 and 3.

identical concentrations of 231011TM, 341011TM, and 34MD1011DM result in similar extents of DNA unwinding, with this extent being greater (by some factor between 1 and 10) than that induced by the same concentration of palmatine. Note that, in this DNA unwinding assay, the extent to which a ligand unwinds the host DNA duplex depends both on the affinity of the ligand for the DNA as well as on the magnitude of its induced DNA unwinding angle. Our viscometric measurements described below indicate that the DNA binding of the protoberberines induces a similar helix unwinding angle with a magnitude of $\approx$11°. In addition, our DNA binding affinity data (summarized below in Table 1) indicate that 231011TM, 341011TM, and 34MD1011DM exhibit similar affinities for salmon testes (ST) DNA, with this affinity being $\approx$3 times greater than that exhibited by palmatine. Thus, the enhanced extent of DNA unwinding induced by 231011TM, 341011TM, and 34MD1011DM relative to palmatine is due to the reduced DNA binding affinity of palmatine relative to the other three protoberberines.

Note that even at a concentration of 100 μM, neither of the four protoberberines unwinds the host DNA to the extent induced by the classical intercalator ethidium bromide (EtBr) at a concentration of only 10 μM (Figure 3). Previous spectroscopic studies by Chou et al. (*24*) yielded an EtBr−ST DNA association constant (K_a) of 1.3 × 10^7 M^{-1} in the presence of 16 mM Na^+. This DNA binding affinity is at least 52−165 times greater than the corresponding proto-

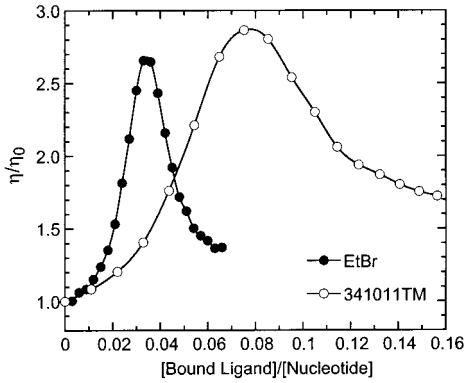

FIGURE 4: Viscometric titrations at 25.7 °C of ΦX-174 RF I DNA with ethidium bromide (filled circles) and 341011TM (open circles). η_0 is the solution viscosity in the absence of ligand, and η/η_0 is the relative solution viscosity. Solution conditions were 1.3 mM Tris-HCl, 5 mM sodium cacodylate, 0.2 mM EDTA, and pH 6.1.

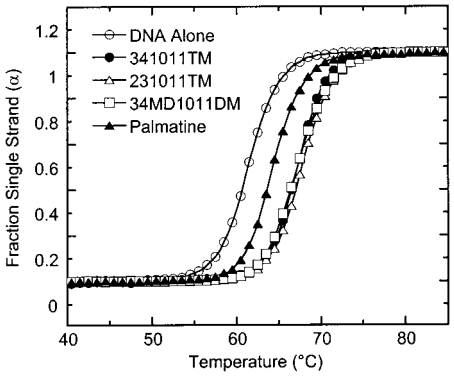

FIGURE 5: UV melting profiles for salmon testes DNA (ST DNA) and its complexes with 231011TM (open triangles), 341011TM (solid circles), 34MD1011DM (open squares), and palmatine (solid triangles) at a [total ligand] to [base pair] ratio (r_{bp}) of 0.5. Solution conditions were 5 mM sodium cacodylate (pH 7.0) and 0.1 mM EDTA. For clarity of presentation, the melting curves were normalized by subtraction of the upper and lower baselines to yield plots of fraction single strand versus temperature (*15*). All the melting profiles were acquired at 260 nm.

berberine−ST DNA association constants (which range from 7.9×10^4 to 2.5×10^5 M^{-1} in the presence of only 3.5 mM Na^+) determined in our studies and described below (see Table 1). In addition, EtBr intercalation is known to unwind duplex DNA by 26° (*25*, *26*). This unwinding angle is significantly larger in magnitude than the protoberberine-induced unwinding angle of 11° revealed by our viscometric studies described in the next section. Hence, the diminished extents to which the protoberberines unwind the host DNA relative to EtBr reflect not only lower DNA binding affinities but also smaller induced unwinding angles.

Viscometric Studies Reveal a Protoberberine-Induced DNA Unwinding Angle of ≈11°. We used viscometric techniques to quantify the DNA unwinding angle (ϕ) induced by protoberberine complexation. In these studies, a negatively supercoiled circular DNA duplex (ΦX-174 RF I) was used as the target for protoberberine binding. Ligand intercalation into circular duplex DNA unwinds negative supercoils, ultimately creating a fully relaxed circular molecule, followed by formation of a positively supercoiled molecule (*27*−*29*). Such ligand-induced changes in tertiary structure are characterized by an increase in viscosity upon unwinding of negative supercoils, followed by a decrease in viscosity with the formation of positive supercoils (*30*). The ratio of *bound* ligand to nucleotide at which the circular DNA molecule is fully relaxed is termed the critical saturation ratio, $\tilde{\nu}$.

Figure 4 shows the effect of either 341011TM or EtBr on the viscosity of a solution containing negatively supercoiled ΦX-174 RF I DNA. Ethidium, a classic intercalating ligand known to unwind duplex DNA by 26° (*25*−*27*, *31*, *32*), was used as a control in this study. Both ethidium and 341011TM result in the expected viscosity profiles for intercalation, with observed $\tilde{\nu}$ values of 0.033 and 0.075, respectively. 231011TM, 34MD1011DM, and palmatine yielded similar viscosity profiles to 341011TM (not shown). Our observed $\tilde{\nu}$ value of 0.033 for ethidium is similar to the values of 0.035 and 0.037 previously reported for the binding of ethidium to pBR322 (*16*) and polyoma virus DNA (*27*), respectively. The helix unwinding angle (ϕ) induced by protoberberine binding can be determined using the following relationship (*33*):

$$\phi_E \tilde{\nu}_E = \phi_P \tilde{\nu}_P \quad (1)$$

ϕ_E and $\tilde{\nu}_E$ reflect the ethidium-induced helix unwinding angle (known to be 26°) and critical saturation ratio, respectively, while ϕ_P and $\tilde{\nu}_P$ are the corresponding protoberberine parameters. Using this approach, we calculate a ϕ_P value of ≈11°. This helix unwinding angle is in excellent agreement with the 10° value reported by the Wilson group for the DNA binding of berberine, a structurally similar protoberberine to those studied here (*34*, *35*).

All Four Protoberberine Analogues Bind to and Enhance the Thermal Stability of Salmon Testes DNA (ST DNA). Figure 5 shows the UV melting profiles for ST DNA in the absence and presence of saturating amounts of 231011TM, 341011TM, 34MD1011DM, and palmatine. Inspection of Figure 5 reveals that the presence of each of the protoberberine analogues enhances the thermal stability of the target DNA duplex. These ligand-induced changes in duplex thermal stability are consistent with all four ligands binding to the target duplex, with a preference for the duplex versus the single-stranded state (*36*, *37*). Further note that the binding of 231011TM, 341011TM, and 34MD1011DM enhances the thermal stability of the host duplex to a similar extent ($\Delta T_m \approx 6$ °C), with this extent being approximately 2-fold greater than that induced by the binding of palmatine ($\Delta T_m \approx 3$ °C). Recall that 231011TM, 341011TM, and 34MD1011DM differ with respect to the identities of the functional moieties on their A-rings, while palmatine differs from 231011TM with respect to the functional groups on the D-ring (see Figure 1). Thus, as measured by differences in ΔT_m, changing the functional groups of the protoberberine D-ring has a greater impact on DNA binding than changing the functional groups of the A-ring.

Note that the extent of duplex thermal enhancement follows the same hierarchy defined above based on our DNA unwinding measurements, namely, 231011TM ≈ 341011TM ≈ 34MD1011DM > palmatine. This correlation between ΔT_m-based and DNA unwinding-based trends also extends to the hierarchy of overall DNA binding affinity, which is presented in the next section.

Relative 231011TM, 341011TM, 34MD1011DM, and Palmatine Binding Affinities for ST DNA Derived from UV Melting Data. We used the ΔT_m method described below to

assess the relative strength of protoberberine binding to ST DNA. Measured ligand-induced changes in the thermal stability of the host DNA (see Figure 5) were used in conjunction with a 2-bp binding site size (n), characteristic of a nearest-neighbor exclusion mode of complexation, to estimate apparent ligand−DNA association constants at T_m (K_{T_m}) using the expression (*36*):

$$\frac{1}{T_{m0}} - \frac{1}{T_m} = \frac{R}{n(\Delta H_{WC})}\ln(1 + K_{T_m}L) \qquad (2)$$

where T_{m0} and T_m are the melting temperatures of the ligand-free and ligand-saturated DNA, respectively; ΔH_{WC} is the enthalpy change for the melting of a Watson−Crick (WC) base pair in the absence of bound ligand [a value we determined independently for the target DNA using differential scanning calorimetry (DSC)]; and L is the free ligand concentration at T_m, which can be estimated by one-half the total ligand concentration. For meaningful comparisons, the calculated apparent binding constants at T_m should be extrapolated to a common reference temperature using the standard relationship:

$$\frac{\partial \ln K}{\partial(1/T)} = -\frac{\Delta H_b}{R} \qquad (3)$$

where ΔH_b is the enthalpy of ligand binding.

Table 1 summarizes the apparent association constants at 25 °C (K_{25}) that we have calculated using eqs 2 and 3 for 231011TM, 341011TM, 34MD1011DM, and palmatine binding to ST DNA. The 231011TM, 341011TM, 34MD1011DM, and palmatine binding enthalpies required for extrapolation of the binding constants to a common reference temperature using eq 3 were determined using isothermal titration calorimetry (ITC). Figure 6 shows representative ITC profiles resulting from eight sequential injections of either 231011TM (panel A) or palmatine (panel B) into a ST DNA solution at a constant temperature of 20 °C. These eight injections resulted in a final [drug]/[base pair] ratio (r_{bp}) of 0.08, with each of the heat burst curves in Figure 6 corresponding to a single ligand injection. The areas under these heat burst curves, as well as those for ST DNA complexation with 341011TM and 34MD1011DM (not shown), were determined by integration to yield the associated injection heats. Note that for each ligand, the eight injection heats were similar in magnitude, an observation consistent with all the injected ligand being bound by the host DNA. These injection heats were divided by the total concentration of injected ligand and averaged to yield the ligand binding enthalpies (ΔH_b) listed in Table 2. It is interesting to compare these enthalpies for protoberberine binding with the enthalpy previously reported (*24*) for the complexation of the classic DNA intercalator, EtBr, with ST DNA (−12.4 kcal/mol). This comparison reveals that the enthalpies of protoberberine−ST DNA complexation observed here, which range from −1.8 to −3.6 kcal/mol (Table 2), are significantly less exothermic (less favorable) than the corresponding binding enthalpy of EtBr. One potential source for this differential enthalpic behavior is that protoberberines engage in fewer enthalpically favorable stacking interactions with the host DNA base pairs than EtBr. Calorimetric, viscometric, and NMR data previously reported by us (*10*) and others (*34*, *38*) are consistent with a model for protoberberine-DNA complexation in which only a portion of the ligand molecule inserts into the DNA helix and engages in stacking interactions with neighboring base pairs.

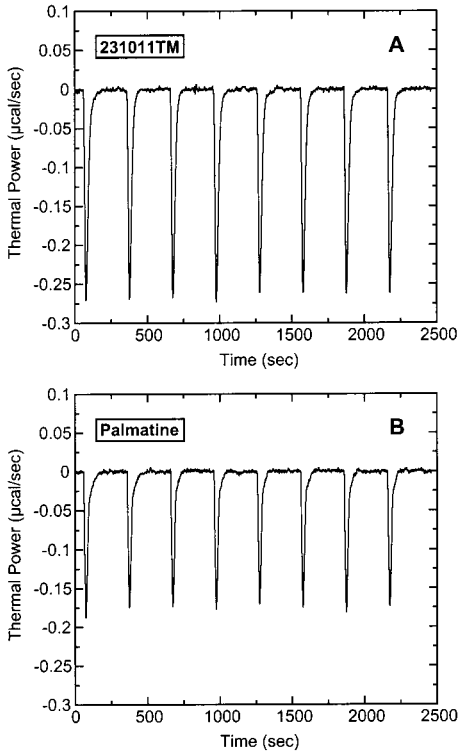

FIGURE 6: ITC profiles at 20 °C for the titration of either 231011TM (A) or palmatine (B) into a 200 μM bp solution of ST DNA. Each heat burst curve is the result of a 5-μL injection from a 500 μM solution of ligand, with all eight injections resulting in a final [drug]/[base pair] ratio (r_{bp}) of 0.08. Solution conditions are as stated in the legend to Figure 5.

Table 2: Calorimetrically Derived Binding Enthalpies (ΔH_b) for the Interactions of 231011TM, 341011TM, 34MD1011DM, and Palmatine with Salmon Testes DNA at 20 °C[a]

ligand	ΔH_b[b] (kcal/mol)
231011TM	-2.8 ± 0.2
341011TM	-3.6 ± 0.2
34MD1011DM	-3.1 ± 0.2
palmatine	-1.8 ± 0.2

[a] Solution conditions are as described in the footnote to Table 1. [b] ΔH_b values were determined as described in the text. Indicated errors correspond to the standard deviation from the mean of at least eight sequential injections that result in a final r_{bp} ratio of 0.08.

Inspection of the data in Table 1 reveals that, at 25 °C, 231011TM, 341011TM, and 34MD1011DM exhibit similar binding affinities for ST DNA ($K_{25} \approx 2 \times 10^5$ M^{-1}). Recall that the A-ring substituents of 231011TM, 341011TM, and 34MD1011DM are 2,3-dimethoxy, 3,4-dimethoxy, and 3,4-methylenedioxy, respectively (see Figure 1), and represent the only structural differences between the three analogues. Thus, changing the A-ring substituents has little or no impact on the affinity of the protoberberine for the host DNA. Further inspection of the data in Table 1 reveals that palmatine binds to ST DNA with an approximately 3-fold lower affinity ($K_{25} \approx 8 \times 10^4$ M^{-1}) than either 231011TM, 341011TM, or 34MD1011DM. The only difference between palmatine and 231011TM is in their D-ring substituents (see Figure 1). Thus, changes in the D-ring substituents of a

Table 3: Thermodynamic Parameters for the Binding of 231011TM, 341011TM, 34MD1011DM, and Palmatine to Salmon Testes DNA[a]

ligand	ΔH_b (kcal/mol)	$T\Delta S_b$[b] (kcal/mol)	ΔG_{b25}[c] (kcal/mol)
231011TM	-2.8 ± 0.2	$+4.5 \pm 0.3$	-7.3 ± 0.1
341011TM	-3.6 ± 0.2	$+3.8 \pm 0.3$	-7.4 ± 0.1
34MD1011DM	-3.1 ± 0.2	$+4.2 \pm 0.3$	-7.3 ± 0.1
palmatine	-1.8 ± 0.2	$+4.9 \pm 0.3$	-6.7 ± 0.1

[a] Solution conditions are as described in the footnote to Table 1. [b] ΔS_b is the binding entropy, as determined using eq 5 in the text and the corresponding values of ΔH_b and ΔG_{b25}. Indicated uncertainties reflect the maximum possible errors in ΔS_b that result from the corresponding uncertainties in ΔH_b and ΔG_{b25}, as propagated through eq 5. [c] ΔG_{b25} is the binding free energy at 25 °C, as determined using eq 4 in the text and the corresponding value of K_{25}. Indicated uncertainties reflect the maximum possible errors in ΔG_{b25} that result from the corresponding uncertainties in K_{25}, as propagated through eq 4.

protoberberine modulate its affinity for DNA, a consequence that contrasts with that noted above for changes in the A-ring functionalities.

DISCUSSION

DNA Unwinding and Thermodynamic Data Reveal that the Protoberberines Bind to Duplex DNA by Intercalation, with this Complexation Being <50% Enthalpy Driven. As noted above, our observation that protoberberine binding unwinds the host DNA duplex by ≈11° is consistent with an intercalative mode of interaction (see Figures 3 and 4). It is of interest to evaluate the thermodynamic driving forces for protoberberine−DNA complexation. Armed with the binding constants listed in Table 1, we have calculated the corresponding binding free energies (ΔG_b) using the standard relationship:

$$\Delta G_b = -RT \ln K \quad (4)$$

These binding free energies, coupled with our calorimetrically derived binding enthalpies listed in Table 2, allow us to calculate the corresponding binding entropies (ΔS_b) using the standard relationship:

$$\Delta S_b = \frac{\Delta H_b - \Delta G_b}{T} \quad (5)$$

These calculations enabled us to generate complete thermodynamic profiles for the binding of the four protoberberines studied here to ST DNA. The resulting profiles are summarized in Table 3. Note that the DNA binding of the protoberberines is between 27 and 49% enthalpy driven, depending on the ligand. In other words, enthalpically favorable interactions provide less than half of the energetic driving force for protoberberine−DNA complexation. By contrast, the Breslauer group has shown that enthalpically favorable interactions provide 80 to 100% of the driving force for the binding of the classic intercalators, EtBr and propidium iodide (PrI), to ST DNA in the presence of 16 mM Na^+ (*24*). One potential explanation for the differences in the thermodynamic driving forces for the DNA binding of the protoberberines relative to EtBr and PrI is that the intercalated protoberberines do not stack with the DNA base pairs as well as EtBr and PrI do. One possible model consistent with this notion is one in which only a portion of the protoberberine molecule intercalates into the host duplex, with the remaining portion protruding out of the helix interior. In such a model, only the inserted portion of the ligand is able to engage in enthalpically favorable stacking interactions with neighboring base pairs. In fact, our computer modeling studies described below reveal such a protoberberine−DNA complex, in which only the C and D rings of the ligand insert into the helical stack.

Comparison of 231011TM, 341011TM, and 34MD1011DM: Modifications of the Protoberberine A-Ring Modulate TOP1 Poisoning While Having a Minimal Impact on DNA Binding. A comparison of the DNA unwinding (Figure 3), UV melting (Figure 5), binding enthalpy (Table 2), and binding affinity (Table 1) data for 231011TM, 341011TM, and 34MD1011DM reveals that these three ligands exhibit similar DNA-binding properties. Note that the structural differences between these analogues are restricted to the chemical substituents of the A-ring (see Figure 1). Thus, modifications of the A-ring have a negligible impact on protoberberine−DNA interactions.

In marked contrast to the similar DNA-binding properties exhibited by 231011TM, 341011TM, and 34MD1011DM, they exhibit differing TOP1 poisoning activities (see Figure 2). Specifically, the TOP1 poisoning efficacies of these three analogues follow the hierarchy: 34MD1011DM > 231011TM ≫ 341011TM. Thus, changing a 2,3-dimethoxy to a 3,4-dimethoxy substituent (compare 231011TM with 341011TM) essentially abolishes TOP1 poisoning activity. However, changing the 3,4-dimethoxy moiety to a 3,4-methylenedioxy substituent not only restores TOP1 poisoning activity (compare 341011TM with 34MD1011DM) but enhances it to a level approximately 10-fold greater than that observed for the 2,3-dimethoxy-substituted molecule (compare 34MD1011DM with 231011TM). These differences in TOP1 poisoning activity cannot be related to differences in DNA binding, since, as noted above, the three analogues exhibit similar DNA-binding properties. Instead, we suggest that the observed differences in TOP1 poisoning activity among the three analogues are due to differences in their abilities to interact with the TOP1 enzyme and stabilize it in the cleavable state. Specifically, the 3,4-dimethoxy substituent of 341011TM may not be tolerated sterically by the enzyme in its cleavable form, thereby rendering this protoberberine analogue unable to poison TOP1. It is reasonable to suggest that the 4-methoxy group of 341011TM may be the only moiety that is not tolerated sterically by the cleavable form of the enzyme, since 231011TM, which, like 341011TM, contains a methoxy group at its 3-position, is able to poison TOP1.

Note that 3,4-methylenedioxy is a less bulky functionality than 3,4-dimethoxy. Hence, the 3,4-methylenedioxy moiety of 34MD1011DM may not only eliminate the steric clash created by the 3,4-dimethoxy substituent of 341011TM, but may engage in favorable interactions with the enzyme, perhaps via the formation of hydrogen bonds involving one or more of its oxygen atoms. Such favorable interactions would result in 34MD1011DM being a more potent TOP1 poison than either 341011TM or 231011TM, as demonstrated by our data. The enhanced TOP1 poisoning efficacy of 34MD1011DM relative to 341011TM is similar to a previously reported structure−activity relationship among the

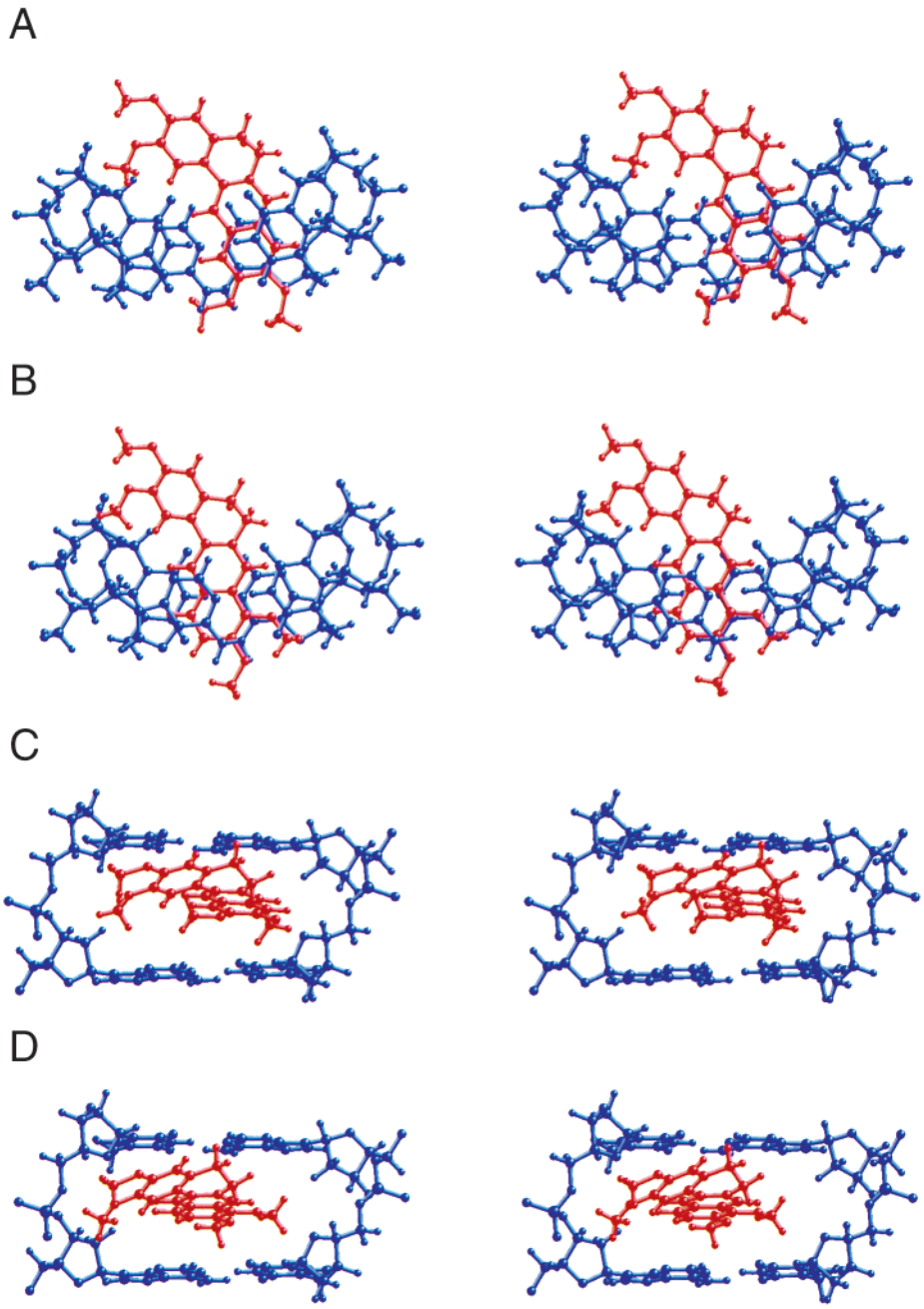

FIGURE 7: Low-energy models for the complexes of 231011TM (panels A and C) and palmatine (panels B and D) with d(ApT)$_n$−d(TpA)$_n$. The DNA is shown in mauve, while the ligand molecules are shown in red. Panels A and B present stereoviews looking down the helical axis of the host DNA duplex. In these views, the upper and lower edges of the DNA correspond to the minor and major grooves, respectively. Panels C and D present stereoviews looking into the DNA major groove. Note the tilting of the A-ring relative to the plane formed by rings C and D.

camptothecin family of compounds (*39*, *40*). This study revealed that 10,11-methylenedioxycamptothecin is a 10-fold more potent TOP1 poison than either 10-methylcamptothecin or camptothecin, with 10,11-dimethoxycamptothecin being completely inactive (*39*, *40*). Although the molecular basis for these differential TOP1 poisoning activities of the camptothecin analogues is still unclear, the similarity between the structure−activity relationships among the camptothecins and the protoberberines suggests that these two classes of compounds may act at a similar site in the ternary (drug−DNA−TOP1) cleavable complex.

Comparison of 231011TM with Palmatine: Transferring a Methoxy Group from the 11- to the 9-Position of the D-Ring Reduces Both DNA Binding Affinity and TOP1 Poisoning Activity. A comparison of the DNA binding data (see Table 1) for 231011TM and palmatine reveals that 231011TM binds to ST DNA with an approximately 3-fold higher affinity than does palmatine. Thus, the transfer of a single methoxy group from the 11- to the 9-position of the D-ring reduces DNA binding affinity by approximately 3-fold. In other words, modifications of the D-ring, unlike modifications of the A-ring, modulate DNA-binding properties. Recall our proposed model for protoberberine−DNA complexation in which only a portion of the ligand molecule inserts into the DNA helix, with the remaining portion protruding out of the helix interior. Our DNA binding data suggest that the D-ring is included in that portion of the ligand that intercalates into the host DNA helix, while the

A-ring is included in that portion of the ligand that protrudes out of the DNA helix interior.

Note that the reduction in the DNA binding affinity of 231011TM upon transference of a methoxy group from the 11- to the 9-position is entirely enthalpic in origin (compare the thermodynamic profiles for the DNA binding of 231011TM and palmatine in Table 3). This observation suggests that a 10,11-dimethoxy substitution on the D-ring may be more sterically compatible with the structural geometry of the duplex intercalation site than a 9,10-dimethoxy substitution. Crystallographic studies (*41*, *42*) on berberine, which, like palmatine, contains a 9,10-dimethoxy substituent, indicate that the two methoxy groups are twisted above and below the plane formed by rings C and D. These displacements of the bulky methoxy groups from the C−D plane may interfere sterically with proper insertion of the D-ring between base pairs, thereby diminishing the extent of ligand−base stacking and, ultimately, reducing duplex binding affinity. To assess the veracity of this hypothesis, we used the computer modeling techniques described in Materials and Methods to derive structural models for the 231011TM−DNA and palmatine−DNA complexes. These computer modeling studies were conducted in two steps. In the first step, we used the MacroModel version 5.0 software and the AMBER* force field (*18*) to derive structural models for 231011TM and palmatine. These structures (not shown) revealed the A-ring to be tilted by ≈25° relative to the plane formed by rings C and D, by virtue of the single bond at the 5,6-position of the B-ring. In the second step, we used these ligand structures to derive models for the structures of the corresponding ligand−DNA complexes. The resulting models are shown in Figure 7. Note that rings C and D of each ligand are inserted between neighboring base pairs, while rings A and B protrude into the minor groove of the host duplex (Figure 7, panels A and B). These observations are consistent with both our DNA unwinding and thermodynamic data. Further inspection of Figure 7 reveals that the extent to which the C- and D-rings are stacked with neighboring base pairs is greater for 231011TM than for palmatine (compare panel A with panel B and panel C with panel D). This observation is consistent with our thermodynamic data (Table 3) as well as our hypothesis that transference of a methoxy group from the 11- to the 9-position diminishes DNA binding affinity by reducing the extent of ligand−base stacking interactions.

Our DNA cleavage data (Figure 2) reveal that 231011TM stimulates TOP1-mediated DNA cleavage, while palmatine does not. Thus, the reduction in DNA binding affinity that accompanies the transfer of a methoxy group from the 11- to the 9-position of the D-ring is correlated with a corresponding reduction in TOP1 poisoning activity. This correlation suggests that modifications of the D-ring that diminish DNA binding affinity also reduce TOP1 poisoning activity.

Both Ligand−DNA and Ligand−Enzyme Interactions Are Potentially Involved in TOP1 Poisoning by Protoberberines. We have shown that modifications of the A- and D-rings can modulate the DNA binding and/or TOP1 poisoning properties of protoberberines. Specifically, modifications of the A-ring modulate TOP1 poisoning activity while having a minimal impact on DNA-binding properties. By contrast, modifications of the D-ring modulate both TOP1 poisoning and DNA-binding properties. These structure−activity relationships are consistent with a model for TOP1 poisoning by protoberberines in which both ligand−DNA and ligand−enzyme interactions are required for stabilization of the ternary (TOP1−DNA−ligand) cleavable complex. In such a model, the C- and D-rings intercalate into the host DNA helix, while the A- and B-rings protrude out of the helix interior, where they are free to interact with specific functional groups on the enzyme. Our computer modeling studies suggest that such ligand−enzyme interactions may occur in the minor groove of the host DNA duplex. It is reasonable to suggest that an ensemble of both ligand−DNA and ligand−enzyme interactions may be of general importance in the poisoning of TOP1 by a broad range of naturally occurring and synthetic ligands. Additional studies currently are underway to assess the specific nature of the ligand−enzyme interactions that are implicated in the poisoning of TOP1 by protoberberines.

ACKNOWLEDGMENT

We are indebted to Dr. Darshan Makhey for his efforts in the synthesis of 231011TM, 341011TM, and 34MD1011DM.

REFERENCES

1. Pantazis, P., Giovanella, B., and Rothenberg, M. L. (1996) *The Camptothecins: From Discovery to the Patient*, pp 1−328, New York Academy of Sciences, New York.
2. Hsiang, Y.-H., Hertzberg, R., Hecht, S., and Liu, L. F. (1985) *J. Biol. Chem. 260*, 14873−14878.
3. Hsiang, Y.-H., Lihou, M. G., and Liu, L. F. (1989) *Cancer Res. 49*, 5077−5082.
4. Porter, S. E., and Champoux, J. J. (1989) *Nucleic Acids Res. 17*, 8521−8532.
5. Leteurtre, F., Fesen, M., Kohlhagen, G., Kohn, K. W., and Pommier, Y. (1993) *Biochemistry 32*, 8955−8962.
6. Pommier, Y., Kohlhagen, G., Kohn, K. W., Leteurtre, F., Wani, M. C., and Wall, M. E. (1995) *Proc. Natl. Acad. Sci. U.S.A. 92*, 8861−8865.
7. Chen, A. Y., and Liu, L. F. (1994) *Annu. Rev. Pharmacol. Toxicol. 34*, 191−218.
8. Bodley, A. L., Liu, L. F., Israel, M., Ramakrishnan, S., Yoshihiro, K., Giuliani, F. C., Kirschenbaum, S., Silber, R., and Potmesil, M. (1989) *Cancer Res. 49*, 5969−5978.
9. Bhakkuni, D. S., and Jain, S. (1986) *The Alkaloids*, Vol. 28, pp 95−181, Academic Press, New York.
10. Pilch, D. S., Yu, C., Makhey, D., LaVoie, E. J., Srinivasan, A. R., Olson, W. K., Sauers, R. R., Breslauer, K. J., Geacintov, N. E., and Liu, L. F. (1997) *Biochemistry 36*, 12542−12553.
11. Gatto, B., Sanders, M. M., Yu, C., Wu, H.-Y., Makhey, D., LaVoie, E. J., and Liu, L. F. (1996) *Cancer Res. 56*, 2795−2800.
12. Makhey, D., Gatto, B., Yu, C., Liu, A., Liu, L. F., and LaVoie, E. J. (1995) *Med. Chem. Res. 5*, 1−12.
13. Makhey, D., Gatto, B., Yu, C., Liu, A., Liu, L. F., and LaVoie, E. J. (1996) *Bioorg. Med. Chem. 4*, 781−791.
14. Chen, A. Y., Yu, C., Bodley, A., Peng, L. F., and Liu, L. F. (1993) *Cancer Res. 53*, 1332−1337.
15. Marky, L. A., and Breslauer, K. J. (1987) *Biopolymers 26*, 1601−1620.
16. Pilch, D. S., Kirolos, M. A., Liu, X., Plum, G. E., and Breslauer, K. J. (1995) *Biochemistry 34*, 9962−9976.
17. Pilch, D. S., Kirolos, M. A., and Breslauer, K. J. (1995) *Biochemistry 34*, 16107−16124.
18. Mohamadi, F., Richards, N. G. J., Guida, W. C., Liskamp, R., Lipton, M., Caufield, C., Chang, G., Hendrickson, T., and Still, W. C. (1990) *J. Comput. Chem. 11*, 440−467.
19. Srinivasan, A. R., and Olson, W. K. (1987) *J. Biomol. Struct. Dyn. 4*, 895−938.

20. Chandrasekaran, R., and Arnott, S. (1989) in *Landolt-Börnstein Numerical Data and Functional Relationships in Science and Technology*, (Saenger, W., Ed.) Group VII, Vol. 1, Nucleic Acids, Subvolume B, pp 31−170, Springer-Verlag, Berlin.
21. Berman, H. M., and Young, P. R. (1981) *Annu. Rev. Biophys. Bioeng. 10*, 87−114.
22. Zhurkin, V. B., Poltev, V. I., and Florent'ev, V. L. (1980) *Molek. Biol. (USSR) 14*, 1116−1130.
23. Poltev, V. I., and Shulyupina, N. V. (1986) *J. Biomol. Struct. Dyn. 3*, 739−765.
24. Chou, W. Y., Marky, L. A., Zaunczkowski, D., and Breslauer, K. J. (1987) *J. Biomol. Struct. Dyn. 5*, 345−359.
25. Wang, J. C. (1974) *J. Mol. Biol. 89*, 783−801.
26. Liu, L. F., and Wang, J. C. (1975) *Biochim. Biophys. Acta 395*, 405−412.
27. Crawford, L. V., and Waring, M. J. (1967) *J. Mol. Biol. 25*, 23−30.
28. Bauer, W., and Vinograd, J. (1968) *J. Mol. Biol. 33*, 141−171.
29. Waring, M. (1971) *Prog. Mol. Subcell. Biol. 2*, 216−231.
30. Révet, B. M. J., Schmir, M., and Vinograd, J. (1971) *Nature New Biol. 229*, 10−13.
31. Waring, M. J. (1966) *Biochim. Biophys. Acta 114*, 234−244.
32. Keller, W. (1975) *Proc. Natl. Acad. Sci. U.S.A. 72*, 4876−4880.
33. Cantor, C. R., and Schimmel, P. R. (1980) *Biophysical Chemistry, Part I: The Conformation of Biological Macromolecules*, pp 311−341, W. H. Freeman, San Francisco.
34. Davidson, M. W., Lopp, I., Alexander, S., and Wilson, W. D. (1977) *Nucleic Acids Res. 4*, 2697−2712.
35. Jones, R. L., Lanier, A. C., Keel, R. A., and Wilson, W. D. (1980) *Nucleic Acids Res. 8*, 1613−1624.
36. Crothers, D. M. (1971) *Biopolymers 10*, 2147−2160.
37. Snyder, J. G., Hartman, N. G., D'Estantoit, B. L., Kennard, O., Remeta, D. P., and Breslauer, K. J. (1989) *Proc. Natl. Acad. Sci. U.S.A. 86*, 3968−3972.
38. Saran, A., Srivastava, S., Coutinho, E., and Maiti, M. (1995) *Indian J. Biochem. Biophys. 32*, 74−77.
39. Hsiang, Y.-H., Liu, L. F., Wall, M. E., Wani, M. C., Nicholas, A. W., Manikumar, G., Kirschenbaum, S., Silber, R., and Potmesil, M. (1989) *Cancer Res. 49*, 4385−4389.
40. Hsiang, Y.-H., Liu, L. F., Wall, M. E., Wani, M. C., Nicholas, A. W., Manikumar, G., Kirschenbaum, S., Silber, R., and Potmesil, M. (1989) *Cancer Res. 49*, 6868.
41. Abdol Abadi, B. E., Moss, D. S., and Palmer, R. A. (1984) *J. Crystallogr. Spectrosc. Res. 14*, 269−281.
42. Kariuki, B. M., and Jones, W. (1995) *Acta Crystallogr. C51*, 1234−1240.

BI000171G